Journal of Organometallic Chemistry 763-764 (2014) 6–13

Contents lists available at ScienceDirect

Journal of Organometallic Chemistry

journal homepage: www.elsevier.com/locate/jorganchem

Coordinated and uncoordinated anion dictated coordination mode of PN(Me)P ligand in Pd(II) complexes and their catalytic applications

Masilamani Tamizmani, Ramakrishna Kankanala, Chinnappan Sivasankar*

Catalysis and Energy Laboratory, Department of Chemistry, Pondicherry University, Puducherry 605014, India

ARTICLE INFO

Article history:
Received 29 January 2014
Received in revised form
8 April 2014
Accepted 9 April 2014

Keywords:
C–N bond cleavage
PNP pincer ligand
Palladium complex
DFT studies
C–C coupling reactions

ABSTRACT

The PN(Me)P ligands based complexes [(η^2-PN(Me)P^{Ph})$PdCl_2$] (**1**), [(η^3-PN(Me)P^{Ph})PdCl](OTf) (**2**) and [(η^3-PNP^{iPr})PdCl] (**3**) (complexes **2** and **3** are pincer type) have been synthesized and characterized using standard analytical methods such as ^{1}H NMR, ^{31}P NMR, elemental analysis, UV–Visible spectroscopy, cyclic voltammetry and single-crystal X-ray crystallography. Formation of complexes **1** and **2** were observed under two different reaction conditions and learned about how the anions can dictate the coordination mode of PNP ligand to have different hapticity to offer different complexes. More importantly, isolation of complexes **1** and **2** filled the gap in PNP–Pd chemistry. DFT calculations have been carried out to understand the C–N bond cleavage of PN(Me)P ligand when –Ph and –^{i}Pr substituent introduced on the phosphorous. The complete reversible pattern of cyclic voltammogram of complex **3** suggests that this complex can be a better catalyst where two different oxidation states involve in the catalytic cycle. We have also performed Heck and Suzuki coupling reactions using complexes **1** and **3** and observed reasonably good yield even at relatively low temperature.

Introduction

The metal-mediated activation and cleavage of strong bonds such as C–H, C–C, C–N, and C–O is one of the most important tools in the modern synthetic organic chemistry [1–10]. Chaudhury et al. reported a C–N bond cleavage reaction assisted by Pd(II) center in alcoholysis of aminal C–N bond [11]. Esteruelas et al. reported the N–H and C–N bond cleavage of pyrimidinic nucleobases and nucleosides assisted by Osmium polyhydride [12]. Bercaw et al. activated and cleaved the C–N bond in nitromethane using palladium acetate and diimine ligand [13]. Recently Zhang et al. studied the C–N bond cleavage of the N-allylpyrrolidine and it was activated by hydrogen-bond, and subsequently produced a stable intermediate Pd(II)-allylic complex [14]. In all the above mentioned complexes the C–N bond cleavage was observed in the organic substrates in the presence of Pd(II) catalysts.

A large number of Pd(II) catalysts are known to promote the above mentioned reactions and most of them are Pd(II) complexes of pincer type ligands [15]. A significant progress has been made in this area during the past twenty five years, particularly with respect to the synthesis of PCP and PNP pincer type transition metal complexes that can cleave C–H, C–C and C–N bonds under mild experimental conditions. Shaw et al. synthesized the first PCP pincer ligand based metal complexes in the middle of 1980s [16], and Milstein et al. [17] developed the chemistry of these complexes. In the recent years many chemists were attracted towards the study of these complexes owing to the efficient catalytic properties of these metal complexes towards the C–H and C–O bond activations, dehydrogenation, hydrogenation and C–C bond forming reactions such as Heck and Suzuki coupling [18–28].

There are several methods to make pincer type transition metal catalysts; nevertheless a widely used method is cleavage of C–H/N–H/C–N/P–H/P–C/Si–H bond in the pincer type ligands to yield metal bound PCP/PNP/PPP/PSiP type of complexes [29–41]. Ozerov et al. have studied a possibility of C–N bond cleavage in neutral arylamidoamine based PN(Me)P (**A**) and neutral iminodibenzyl based PN(Me)P (**B**) pincer ligands (Fig. 1) at Rh, Ir and Pd metal centers (–PR_2 group is diisopropylphosphine) in which the C–N bond cleavage takes place in the ligand system. In the case of Rh and Ir, the mechanism for the C–N bond cleavage follows the oxidative addition owing to the low oxidation state and less coordination number of Rh and Ir precursors [36]. In a similar way a possibility of C–N bond cleavage at the Pd^{II} center has been

* Corresponding author. Tel.: +91 413 2654709; fax: +91 413 2655987.
E-mail addresses: siva.che@pondiuni.edu.in, drcsivas@gmail.com (C. Sivasankar).

http://dx.doi.org/10.1016/j.jorganchem.2014.04.011
0022-328X/

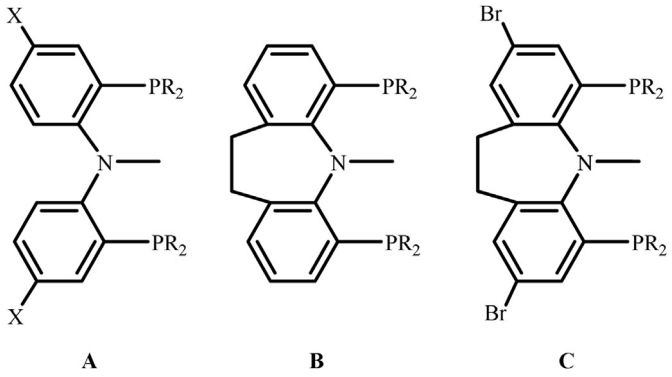

Fig. 1. Ligand systems.

reported with ligands **A** and **B** in which the $-PR_2$ group is diisopropylphosphine. Nevertheless, when the $-PR_2$ group is diphenylphosphine, the product was unidentified [9].

In this regard, in order to gain more insight to understand the C–N bond cleavage at the Pd(II) center, we have synthesized bromine substituted ligand type **C** (Fig. 1). We have used different R groups on the phosphine to isolate certain important complexes which are missing in the PNP–Pd chemistry and also to understand more about the C–N bond cleavage. We have used DFT calculations to understand why the C–N bond cleavage is not observed for diphenyl substituted phosphine ligand while diisopropyl substituted phosphine ligand displaces the C–N bond cleavage. Apart from these studies, we have also studied the catalytic activity of complexes **1** and **3** towards the Mizoroki–Heck and Suzuki coupling reaction.

Results and discussion

Ligands **L1** and **L2** (belong to ligand type **C** in Fig. 1) were synthesized (Scheme 1) using modified literature procedure and characterized by ^1H and ^{31}P NMR spectroscopy techniques. The ligand **L1** is found to be an air and moisture stable while **L2** is not. For ligand **L1**, the ^1H NMR spectrum shows a single peak at 2.74 ppm for N–Me protons and a pair of multiplets at 2.65 ppm and 2.16 ppm for $-CH_2-CH_2-$ linker and the aromatic protons appeared between 7.50 and 6.92 ppm. The $^{31}P\{^1H\}$ NMR spectrum of ligand **L1** shows a single peak at δ −18.34 ppm in $CDCl_3$. These spectral data confirmed the formation of **L1**. The NMR spectral data of ligand **L2** is comparable with the literature data [36].

*Complexation of **L1** and **L2** with [(COD)PdCl$_2$] (COD = cyclooctadiene)*

The reaction of PN(Me)P^{Ph} (**L1**) with [(COD)$PdCl_2$] in toluene at 100 °C for 1.5 h afford [(η^2-PN(Me)P^{Ph})$PdCl_2$] (**1**) as a yellow solid (yield 80%) (Scheme 2). The ^1H NMR spectrum of complex **1** display a single peak at 3.88 ppm for N–Me group and a pair of multiplets at 3.07 ppm and 3.04 ppm for $-CH_2-CH_2-$ protons respectively. The $^{31}P\{^1H\}$ NMR spectrum of complex **1** displays a single peak at δ 22.04 ppm in $CDCl_3$ indicates that the $-PPh_2$ is coordinated with the Pd(II). These spectral data indicate that the complex **1** is formed without C–N bond cleavage and the PN(Me)P ligand behaves as a bidentate ligand (η^2) without the participation of N–Me coordination. The solid state structure of complex **1** was determined using a single-crystal X-ray diffraction studies (Fig. 2). The Pd–Cl1 bond and Pd–Cl2 bond distances are found to be 2.331(2)Å and 2.352(2)Å respectively. The P2–Pd–Cl1 and P1–Pd–Cl2 bond angles are found to be 172.98° and 171.47° respectively. These structural features indicate that the geometry around the central metal ion Pd is square planar.

The reaction of complex **1** with one equivalent of silver triflate in a dichloromethane solution at room temperature for 6 h afford [η^3-PN(Me)P^{Ph}PdCl](OTf) (**2**) (Scheme 2). The formation of complex **2** was confirmed by NMR and X-ray crystallography techniques. The ^1H NMR spectrum of complex **2** displays a pair of multiplets at 3.16 ppm and 3.72 ppm for $-CH_2-CH_2-$ methyl protons and a single peak at 3.96 ppm for N–Me methyl protons. The $^{31}P\{^1H\}$ NMR spectrum of complex **2** displays a single peak at 28.31 ppm in $CDCl_3$. These spectral data indicate that the complex **2** is entirely different from complex **1**. The solid state structure of complex **2** was determined using a single-crystal X-ray diffraction studies (Fig. 3). The Pd–Cl and the Pd–N bond distances are found to be 2.297 Å and 2.180 Å respectively. The N–Me bond distance (1.526 Å) is increased after binding with Pd when compared to the free N–Me bond distance (1.464 Å in complex **1**). The P2–Pd–P1 and N–Pd–Cl bond angles are found to be 171.83° and 176.85° respectively (Table 1). These structural features indicate that the geometry around the central metal ion is square planar and it can be noted that the N–Me fragment of PNP ligand coordinated to the Pd center without undergoing C–N bond cleavage. The employed anions such as OTf^- and Cl^- dictated or controlled the PN(Me)P^{Ph} ligand (**L1**) to change its hapticity from η^2 to η^3 in the presence of respective anions to yield two different complexes **1** and **2**, and demonstrated that how one can synthesize a complex with desired hapticity for a particular application.

Reaction between PN(Me)P^{iPr} (**L2**) and [(COD)$PdCl_2$] in toluene or in acetonitrile solution at 70 °C for 1.5 h afford [η^3-PNP^{iPr}PdCl] (**3**) as a red-orange solid (yield 90%) (Scheme 3). The formation of complex **3** was confirmed by NMR and X-ray crystallography techniques. The ^1H NMR spectrum of complex **3** displays a pair of multiplets at 1.42 ppm and 1.27 ppm for $-CH(Me)_2$ methyl protons and a multiplet at 2.55 ppm for $-CH(Me)_2$ methylene protons and a single peak at 3.81 ppm for $-CH_2-CH_2-$ protons. The $^{31}P\{^1H\}$ NMR spectrum of complex **3** displays a single peak at 49.53 ppm in $CDCl_3$. These spectral data indicate that the complex **3** is formed via H_3C–N bond cleavage and PNP ligand behave as a tridentate ligand (η^3) by producing CH_3Cl as a side product. The solid state structure

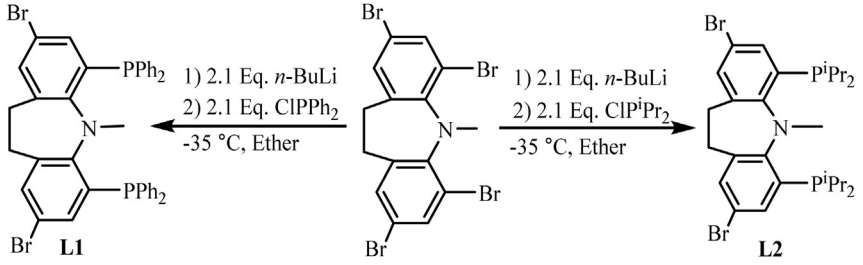

Scheme 1. Synthesis of PN(Me)P^{Ph} (**L1**) and PN(Me)P^{iPr} (**L2**).

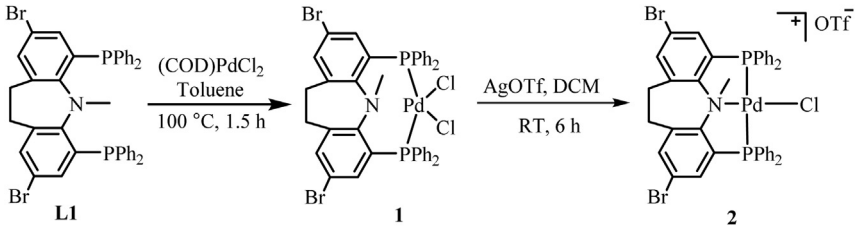

Scheme 2. Synthesis of $[(\eta^2\text{-PN(Me)P}^{Ph})PdCl_2]$ (**1**) and $[(\eta^3\text{-PN(Me)P}^{Ph})PdCl](OTf)$ (**2**).

of complex **3** was determined using a single-crystal X-ray diffraction studies (Fig. 4). The solid state structure of complex **3** shows that the Pd–N1 bond distance is found to be 2.063(3) Å. The Pd–P1 and Pd–P2 distances are found to be 2.2745(1) Å and 2.2757(1) Å respectively. The bond angle of N1–Pd–Cl1 and P1–Pd–P2 are found to be 177.9° and 167.4° respectively. The geometry around the Pd center is found to be square planar. These observed bond distances and bond angles are comparable with the halogen free PNP complex of Pd(II) [36].

The C–N bond cleavage was observed when the $-PR_2$ group is diisopropylphosphine to yield PNP (η^3) coordinated complex **3**. On the other hand the C–N bond cleavage was not observed when the $-PR_2$ group is diphenylphosphine and the $PN(Me)P^{Ph}$ ligand behaves as a bidentate (η^2) and tridentate (η^3), nevertheless the binding fashion of this ligand is also controlled by the other ancillary ligands (complexes **1** and **2**), in this case Cl^- and OTf^-. Although the –Br substitution does not alter the structural features of complex **3**, the bromine substituent on the iminodibenzyl ring enabled us to isolate and characterize some novel missing complexes in the PNP–Pd chemistry. Previously complexes **1** and **2** were expected to form with similar ligands, nevertheless not been isolated in the literature [9,36].

Electronic spectroscopy

The UV–Visible spectra of a dilute solution of complexes **1**–**3** have been recorded in dichloromethane (Fig. 5 and Table 2). The complex **1** shows a strong absorption band at 265 nm and relatively weak absorption band at 431 nm. The corresponding tricoordinate complex **2** shows two medium intense absorption bands at 327 nm and 380 nm. The complex **3** shows an intense absorption band at 334 nm and relatively weak intense band at 431 nm. The absorption bands centered around 250–350 nm can be attributed to the ligand centered $\pi-\pi^*$ transition while the weak bands centered around 400–500 nm can be attributed to the d–d transition for the square planar geometry in their respective complexes **1**–**3**.

Electrochemistry

In order to understand the redox nature of complexes **1** and **3**, the cyclic voltammogram (CV) of complexes **1** and **3** have been recorded in acetonitrile solution (0.5 mM) with 0.1 M Bu_4NPF_6 as an electrolyte at a Pt working electrode with scan rate 50 mV (Fig. 6). The cyclic voltammogram of complex **1** reveals the one electron reversible reduction at −0.89 V. The cyclic voltammogram of complex **3** shows the one electron reversible oxidation at 0.8 V and one electron quasi-reduction at −1.2 V. These results indicate that the $-P^iPr_2$ ligand stabilizes higher oxidation state of $Pd(Pd^{II/III})$ and suggests that the complex **3** can be used as a catalyst in which two different oxidation states involve in the catalytic cycle. Nevertheless complex **1** can be a moderate catalyst. The observed redox potential for complexes **1** and **3** does not match with the reported oxidation potential in the literature for the similar type of ligand therefore the ligand in complexes **1** and **3** might be stable towards the oxidation [42,43].

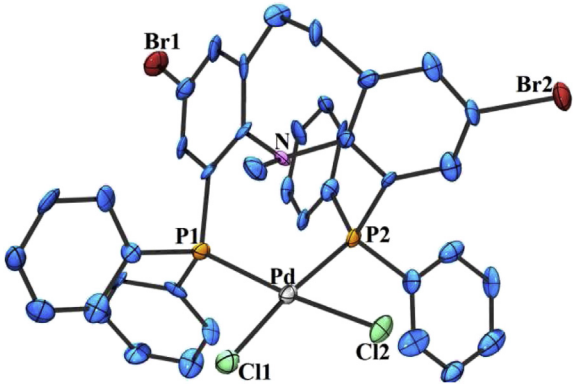

Fig. 2. ORTEP drawing (50% probability ellipsoids) of the $[(\eta^2\text{-PN(Me)P}^{Ph})PdCl_2]$ (**1**). Omitted for clarity: solvated bromobenzene, all H atoms. Selected bond distances (Å): Pd–P1, 2.260(2); Pd–P2, 2.272(2); Pd–Cl2, 2.331(2); Pd–Cl1, 2.352(2); N–C(Methyl), 1.464(10). Selected bond angles (°): P2–Pd–P1, 96.54(9); P1–Pd–Cl2, 172.98(9); P1–Pd–Cl1, 83.34(8); P2–Pd–Cl2, 90.46(9); P2–Pd–Cl1, 171.47(8); Cl1–Pd–Cl2, 89.68(9).

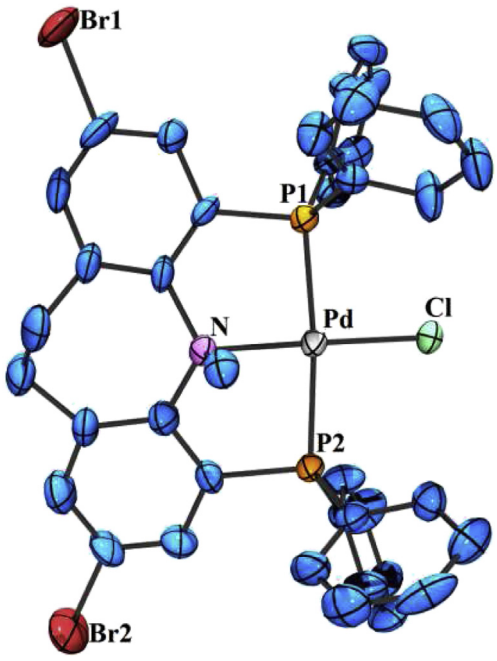

Fig. 3. ORTEP drawing (50% probability ellipsoids) of the $[(\eta^3\text{-PN(Me)P}^{Ph})PdCl](OTf)$ (**2**). Omitted for clarity: solvated dichloromethane, all H atoms. Selected bond distances (Å): Pd–P2, 2.246(3); Pd–P1, 2.250(6); Pd–Cl1, 2.299(8); Pd–N, 2.171(4); N–C (Methyl), 1.526(7). Selected bond angles (°): P2–Pd–P1,171.83(5); P2–Pd–Cl1, 94.22(5); P1–Pd–Cl1, 93.51(5); N–Pd–Cl1, 176.85(1).

Table 1
Experimental and calculated geometrical parameters of complexes **1**–**3**.

	Bond length (Å) or angle (°)	Exp. value	Cal. value
Complex 1	Pd–Cl2	2.331(2)	2.381
	Pd–Cl1	2.352(2)	2.407
	Pd–P1	2.260(2)	2.354
	Pd–P2	2.272(2)	2.375
	P1–Pd–Cl2	172.98(9)	170.59
	P2–Pd–Cl1	171.47(8)	163.71
	Cl1–Pd–Cl2	89.68(9)	89.17
Complex 2	Pd–P2	2.246(3)	2.308
	Pd–P1	2.250(6)	2.302
	Pd–Cl	2.299(8)	2.342
	Pd–N	2.171(4)	2.262
	N–Pd–Cl	176.85(1)	172.62
	P2–Pd–Cl	94.22(5)	93.30
	P1–Pd–Cl	93.51(5)	94.23
Complex 3	Pd–N	2.063(3)	2.121
	Pd–Cl	2.309(5)	2.379
	Pd–P2	2.275(7)	2.316
	Pd–P1	2.274(5)	2.316
	N–Pd–Cl	177.91(9)	179.0
	P1–Pd–Cl	96.91(5)	95.35
	P2–Pd–Cl	95.64(4)	95.56

Catalysis

Pd complexes **1** and **3** have been used for C–C bond formation reactions such as Mizoroki–Heck (Scheme 4) and Suzuki–Miyaura (Scheme 5) coupling reactions. For Mizoroki–Heck coupling reaction, we have chosen aryl halides (iodo & bromo derivatives) and *tert*-butyl acrylate as coupling pairs. As summarized in Table 3, the catalyst **3** produced relatively more yield than the catalyst **1** as reflected in the CV, the product yield is also observed to be strongly depended upon the nature of the substitution on the aryl group. In the case of para-substituted iodobenzene (entry 1 and 2 in Table 3), the product yield is more when compared to the un-substituted iodobenzene (entry 3 and 4 in Table 3). The product yield is further reduced when bromobenzene was used (entry 5 and 6 in Table 3). However the presence of –OMe group at the para position of the phenyl ring increased the yield slightly (entry 7 and 8 in Table 3). The turn over number (TON) has been calculated for all the reactions (Table 3). The TON for 4-MeC_6H_4I is found to be more with catalyst **3** when compared with the catalyst **1**. Nevertheless for all other substituents the TON is found to be reasonable. The catalytic activity of catalysts **1** and **3** is found to be reasonable for Heck coupling reaction because of the even less catalyst load is sufficient to isolate reasonably good yield.

We have chosen boronic acid and aryl halides (iodo & bromo derivatives) for Suzuki-Miyaura coupling reaction. The catalyst **3** is active even at 80 °C but catalyst **1** is active only at 110 °C (Table 4). Relatively more yield was observed for both catalysts **1** and **3** when 4-MeC_6H_4I was used (entry 1, 2 in Table 4). Moderate yield was isolated for C_6H_5Br and 4-MeOC_6H_4Br (entry 3, 4 in Table 4). In all the cases iodo-substituted aryl halides were found to be more reactive than the bromo-substituted aryl halides. From Tables 3 and 4, it can be noted that the complexes **1** and **3** may be useful catalysts for the C–C bond formation reactions even at relatively low temperature.

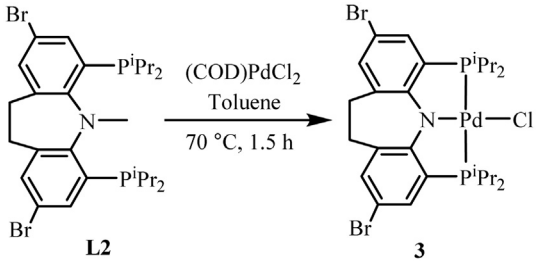

Scheme 3. Synthesis of η^3-PNP^{iPr}PdCl (**3**).

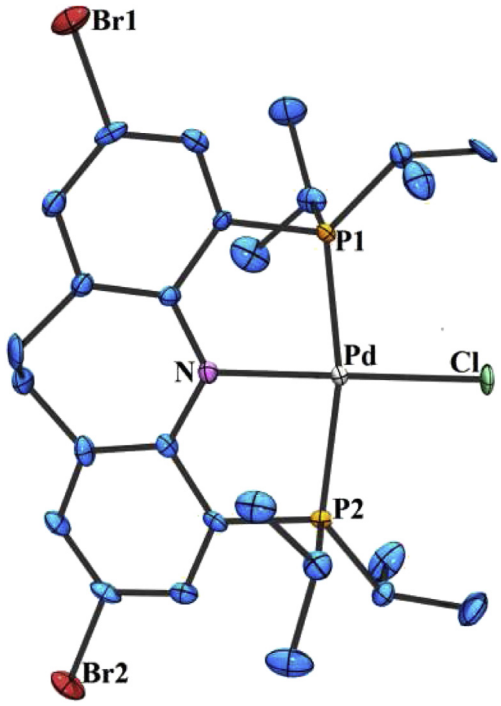

Fig. 4. ORTEP drawing (50% probability ellipsoids) of the [(η^3-PNP^{iPr})PdCl] (**3**). Omitted for clarity: solvated bromobenzene, all H atoms. Selected bond distances (Å): Pd–N1, 2.063(3); Pd–P2, 2.2757(11); Pd–P1, 2.2745(11); Pd–Cl1, 2.3095(10). Selected bond angles [°]: P2–Pd–Cl1, 95.64(4); P1–Pd–P2, 167.45(4); P1–Pd–Cl1, 96.91(4); N1–Pd–Cl1, 177.91(9); N1–Pd–P2, 84.13(9); N1–Pd–P1, 83.33(9).

DFT studies

In order to understand why the complex **1** ([(η^2-PN(Me)P^{Ph})$PdCl_2$] in Eq. (1)) is formed over complex **1a** ([(η^3-PNP^{Ph})PdCl] in Eq. (3)) via C–N bond cleavage with phenyl substituted phosphine

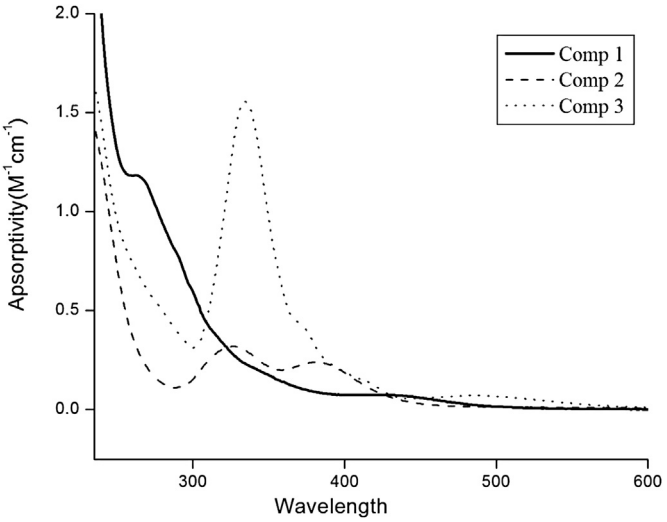

Fig. 5. UV–Visible spectra of complexes **1**–**3** in dichloromethane.

Table 2
UV–Visible data of complexes **1**–**3** in dichloromethane.

Complex	λ_{max} (nm)	ε_{max} (M^{-1} cm^{-1})
Complex **1**	265.0 (S), 431.0 (W)	0.313, 0.24
Complex **2**	327.0 (m), 380.0 (m)	1.16, 0.074
Complex **3**	334.0 (S), 488.0 (W)	1.55, 0.066

in the presence of $[(COD)PdCl_2]$, DFT calculations have been performed. We have used ligands **L1** and **L2** and their complexes (**1**, **2** and **3**) without any simplification for the calculations. The fully optimized structures of all the above mentioned systems can be seen in the supporting information (Fig. S1). We observed a good agreement between calculated structural parameters with the experimentally observed structural parameters (Table 1).

$$L1 + [(COD)PdCl_2] \rightarrow \left[\eta^2 - PN(Me)P^{Ph}PdCl_2\right] (\mathbf{1}) + COD \quad \Delta G = -12.49 \tag{1}$$

$$\left[\eta^2 - PN(Me)P^{Ph}PdCl_2\right](\mathbf{1}) \xrightarrow{AgOTF} \left[\eta^3 - PN(Me)P^{Ph}PdCl\right](OTf)(\mathbf{2}) + AgCl \quad \Delta G = -9.49 \tag{2}$$

$$L1 + [(COD)PdCl_2] \rightarrow \left[\eta^3 - PNP^{Ph}PdCl\right](1a) + COD + CH_3Cl \quad \Delta G = +30.69 \tag{3}$$

$$L2 + [(COD)PdCl_2] \rightarrow \left[\eta^3 - PNP^{iPr}PdCl\right](\mathbf{3}) + COD + CH_3Cl \quad \Delta G = -67.80 \tag{4}$$

We have calculated ΔG for the formation of complex **1** ($[(\eta^2$-$PN(Me)P^{Ph})PdCl_2]$) and found to be exergonic ($\Delta G = -12.49$ kcal/mol) in nature (Eq. (1)). The ΔG for the formation of complex **2** ($[(\eta^3$-$PN(Me)P^{Ph})PdCl](OTf)$) (η^3-$PN(Me)P^{Ph}$ of **L1** without C–N bond cleavage) is also calculated to be exergonic ($\Delta G = -9.49$ kcal/mol) in nature (Eq. (2)) nevertheless, the magnitude is slightly less when compared to the ΔG formation of complex **1**. We have also calculated the ΔG for the formation of hypothetical complex **1a** (η^3-PNP complex of **L1** via C–N bond cleavage) and found to be highly endergonic ($\Delta G = +30.69$ kcal/mol) in nature (Eq. (3)). These calculated ΔG values clearly indicate that the formation of complex **1a** is not thermodynamically feasible over the formation of complexes $[(\eta^2$-$PN(Me)P^{Ph})PdCl_2]$ (**1**) and $[(\eta^3$-$PN(Me)P^{Ph})PdCl](OTf)$ (**2**) therefore the N–Me bond cleavage is not possible in ligand **L1**. The ΔG for the formation of complex **3** is calculated to be highly exergonic ($\Delta G = -67.80$ kcal/mol) in nature (Eq. (4)) therefore the C–N bond cleavage is possible in ligand **L2**.

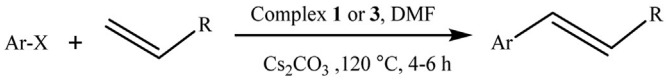

Scheme 4. Mizoroki–Heck coupling reaction.

Conclusion

Reactions of PN(Me)P type ligands **L1** and **L2** with $[(COD)PdCl_2]$ produced complexes $[(\eta^2$-$PN(Me)P^{Ph})PdCl_2]$ (**1**), $[(\eta^3$-$PN(Me)P^{Ph})PdCl](OTf)$ (**2**) and $[(\eta^3$-$PNP^{iPr})PdCl]$ (**3**) under different reaction conditions. Complexes **1**–**3** have been characterized using standard techniques such as ^1H NMR, ^{31}P NMR, elemental analysis, UV–Visible spectroscopy, cyclic voltammetry and single-crystal structural determinations. We also observed that the –Ph substituted PN(Me)P ligand is failed to undergo C–N bond cleavage while $-^iPr$ substituted PN(Me)P ligand followed C–N bond cleavage. Owing to this difference in the reactivity/nature of two different PN(Me)P ligands, we observed η^2 and η^3coordination mode for these ligands (**L1** and **L2**) in complexes **1** and **3** respectively. On the other hand the coordination mode of **L1** changed from η^2 to η^3 without C–N bond cleavage when the Cl^- ion was removed from the Pd in complex **1** by the addition of AgOTf. DFT calculations suggest that the formation of complexes **1**–**3** are thermodynamically feasible nevertheless the C–N bond cleavage is not possible with ligand **L1** to yield complex **1a**. The CV of complex **3** suggests that this complex can be a better catalyst where two different oxidation states involve in the catalytic cycle. Complexes **1** and **3** are found to be suitable to promote Heck and Suzuki coupling reactions to form new C–C bonds even at low temperature. More catalytic studies using complexes **1**–**3** are under investigation.

Experimental section

General considerations

Unless specified otherwise, all manipulations were performed under nitrogen atmosphere using standard Schlenk line techniques. Toluene, diethyl ether, C_6D_6 and THF were dried and distilled over Na/Ph_2CO and stored in an N_2-filled glove box. $CDCl_3$, DCM, Acetonitrile and Bromobenzene were dried and then distilled or vacuum transferred over CaH_2. Chlorodiisopropylphosphine, Chlorodiphenylphosphine and $[(COD)PdCl_2]$ were purchased from Aldrich and used without further purification. *N*-Methyl-tetrabromoiminodibenzyl was prepared

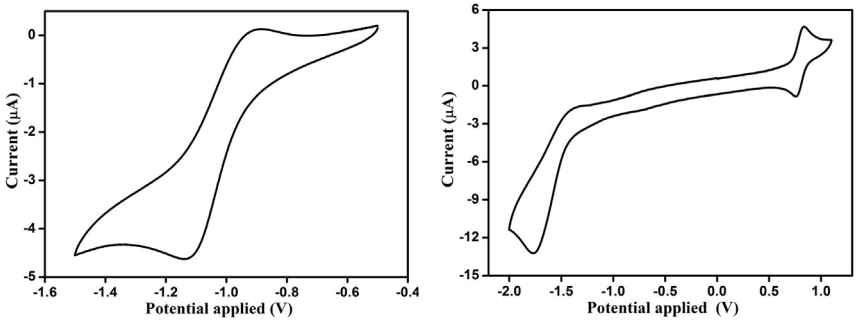

$[(\eta^2$-$PN(Me)P^{Ph})PdCl_2]$ (**1**) $[(PNP^{iPr})PdCl]$ (**3**)

Fig. 6. Cyclic voltammetry of complexes **1**–**3** in acetonitrile (0.5 mM) measured at 298 K with a 0.1 M Bu_4NPF_6 solution at a Pt working electrode (scan rate 50 mV s^{-1}).

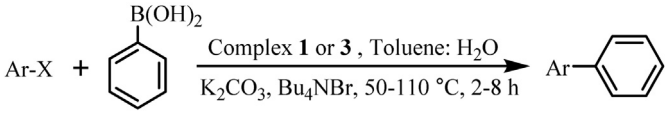

Scheme 5. Suzuki–Muyaura coupling reaction.

according to the literature procedure. NMR spectra were recorded on a Bruker 400 MHz (^{1}H NMR, 400 MHz; ^{13}C NMR, 100.62 MHz; ^{31}P NMR, 161.822 MHz) spectrometer. For ^{1}H NMR and ^{13}C NMR spectra, the residual solvent peak was used as an internal reference. ^{31}P NMR spectra were referenced externally using 85% H_3PO_4 at δ 0 ppm.

Synthesis

*Synthesis of PN(Me)P^{Ph} (**L1**)*

Under an atmosphere of nitrogen, *n*-BuLi (4.0 mL of 1.6 M solution in hexane, 6.38 mmol) was slowly added to the suspension of *N*-methyl tetrabromoiminodibenzyl (1.6 g, 3.04 mmol) in 30 mL of Et_2O at −35 °C. The mixture was stirred for 2 h at room temperature. The solution was cooled to −35 °C and chlorodiphenylphosphine (1.14 g, 6.38 mmol) was added and it was stirred for overnight at room temperature. The volatiles were removed in vacuo and the residue was re-dissolved with ether and filtered. The resulting solution was evaporated in vacuo to yield pale yellowish oil. This oil was treated with methanol to produce a white solid and the solid was collected by filtration. Yield: 1.23 g (55%). ^{1}H NMR ($CDCl_3$): δ 7.50 (m, 4H, Ar–H), 7.32 (m, 2H, Ar–H), 7.25 (m, 4H, Ar–H), 7.10–6.92 (m, 14H, Ar–H), 2.74 (s, 3H, N–Me), 2.65 (m, 2H, CH_2CH_2), 2.16 (m, 2H, CH_2CH_2). ^{31}P{^{1}H} NMR ($CDCl_3$): δ −18.34 (s). ^{13}C NMR ($CDCl_3$): δ 151.9, 142.2, 141.4, 140.1, 138.2, 136.9, 134.9, 134.2, 133.7, 128.9, 128.6, 120.1, 48.4 (t, N–Me), 32.2 (s, $-CH_2CH_2-$). Anal. Calcd. for $C_{39}H_{31}Br_2NP_2$: C, 63.69; H, 4.25; N, 1.90. Found: C, 63.49; H, 4.19; N, 1.63.

*Synthesis of PN(Me)P^{iPr} (**L2**)*

Under an atmosphere of nitrogen, *n*-BuLi (6.0 mL of 1.6 M solution in hexanes, 9.6 mmol) was slowly added to the suspension of N-methyl tetrabromoiminodibenzyl (2.4 g, 4.5 mmol) in 30 mL of Et_2O at −35 °C. The mixture was warm up to room temperature and stirred for 2 h. Then the reaction mixture was cooled to −35 °C and chlorodiisopropylphosphine (1.46 g, 9.6 mmol) was added and it was stirred for overnight at room temperature. The volatiles were removed in vacuo, and the residue was re-dissolved with ether and filtered. The filtrate was treated with silica gel and stirred for 30 min and then the solids were filtered off. The resulting solution was evaporated in vacuo to afford pale yellowish oil. This oil was treated with methanol to produce a white solid and the solid was collected by filtration. Yield: 1.72 g (64%). ^{1}H NMR ($CDCl_3$): δ 7.38 (d, 2H, Ar–H), 7.19 (d, 2H, Ar–H), 3.31 (s, 3H, N–Me), 3.24 (m, 2H, $-CH_2-CH_2-$), 2.73 (m, 2H, $-CH_2-CH_2-$). 2.04 (m, 4H, $-CH(Me)_2$), 1.25–1.20 (m, 6H, $-CH(Me)_2$), 1.20–1.19 (m, 6H, $-CH(Me)_2$), 1.19–1.15 (m, 6H, $-CH(Me)_2$), 1.13–1.07 (m, 6H, $-CH(Me)_2$). ^{13}C NMR ($CDCl_3$): δ 153.4, 141.7, 141.3, 137.2, 135.1, 134.1, 133.2, 118.5 (Ph), 51.1 (t, N–Me), 33.11 (s, $-CH_2CH_2-$), 26.8, 25.9, 22.5, 21.4, 20.29 (–Me of ^{i}Pr), 19.9, 14.2 (CH of ^{i}Pr). ^{31}P{^{1}H} NMR ($CDCl_3$): δ −8.34 (s). Anal. Calcd. for $C_{27}H_{39}Br_2NP_2$: C, 54.11; H, 6.56; N, 2.34. Found: C, 54.23; H, 6.48; N, 2.17.

*Synthesis of [(η^2-PN(Me)P^{Ph})PdCl$_2$] (**1**)*

[(COD)PdCl$_2$] (50 mg, 0.175 mmol) was added to a solution of **L2** (128 mg, 0.175 mmol) in 10 mL of toluene with stirring and the color of the solution rapidly changed to yellow orange, it was stirred for 30 min at room temperature. Then the mixture was heated at 100 °C for 1.5 h while stirring and then the resulting yellow solid was filtered and washed with pentane. Yield: 147.0 mg (92%).^{1}H NMR ($CDCl_3$):δ 7.39–7.37 (m, 6H, Ar–H), 7.40–7.36 (m, 2H Ar–H), 7.32–7.28 (m, 4H, Ar–H), 7.20–7.17 (m, 4H, Ar–H), 6.87–6.84 (m, 8H, Ar–H), 3.87 (s, 3H, N–Me), 3.75–3.68 (m, 2H, $-CH_2CH_2-$), 3.04–2.97 (m, 2H, $-CH_2CH_2-$). ^{31}P{^{1}H} NMR ($CDCl_3$): δ 22.04 (s). ^{13}C NMR ($CDCl_3$): δ 149.8, 143.2, 136.7, 136.5(t), 134.12(t), 133.54(s), 131.08, 130.45, 129.17, 128.36, 128.06(t), 127.9, 121.21(t), 50.06 (s, N–Me), 31.72(s, $-CH_2CH_2-$). Anal. Calcd. for $C_{39}H_{31}Br_2Cl_2NP_2Pd$: C, 51.32; H, 3.42; N, 1.53. Found: C, 51.20; H, 3.28; N, 1.40.

*Synthesis of [(η^3-PN(Me)P^{Ph})PdCl](OTf) (**2**)*

Silver triflate (37 mg, 0.14 mmol) was added to a solution of **1** (120 mg, 0.13 mmol) in 10 mL of dichloromethane with stirring and the color of the solution immediately changed to orange, it was stirred for 6 h at room temperature. Then the mixture is filtered and evacuated completely. Yield: 80.0 mg (53%). ^{1}H NMR ($CDCl_3$):δ 7.69–7.54 (m, 14H, Ar–H), 7.53–7.49 (m, 6H, Ar–H) 7.25–7.21 (m, 2H, Ar–H), 7.09–7.05 (m, 2H, Ar–H), 3.96 (s, 3H, N–Me), 3.72–3.65 (m, 2H, $-CH_2CH_2-$), 3.18–3.12 (m, 2H, $-CH_2CH_2-$). ^{31}P{^{1}H} NMR ($CDCl_3$): δ 28.31 (s). ^{13}C NMR ($CDCl_3$): δ 142.7, 142.1 (t), 140.9, 137.5, 136.1 (t), 134.3 (t), 133.2, 133.0, 130.3 (t), 129.7 (t), 126.2, 125.9, 125.3, 124.1 (t) (Ph), 78.6 (t, $-CF_3$), 62.9 (s, N–Me), 34.7 (s, $-CH_2CH_2-$). Anal. Calcd. for $C_{40}H_{31}Br_2ClF_3NO_3P_2PdS$: C, 46.81; H, 3.04; N, 1.36. Found: C, 46.68; H, 2.98; N, 1.19.

*Synthesis of [(η^3-PNP^{iPr})PdCl] (**3**)*

[(COD)PdCl$_2$] (58 mg, 0.203 mmol) was added to a solution of **L2** (120.61 mg, 0.202 mmol) in 10 mL of acetonitrile with stirring, and

Table 3
Summary of Mizoroki–Heck coupling reaction results.

Entry[a]	Catalyst (mmol) × 10^{-5}	Substrates		Time (h)	Yield	TON
		Ar–X	R			
1	0.2 (**1**)	4-MeC$_6$H$_4$I	–COO^{t}Bu	4	96%	355,500
2	0.2 (**3**)	4-MeC$_6$H$_4$I	–COO^{t}Bu	4	89%	404,500
3	1.0 (**1**)	C$_6$H$_5$I	–COO^{t}Bu	4	76%	58,500
4	1.0 (**3**)	C$_6$H$_5$I	–COO^{t}Bu	4	68%	61,800
5	1.0 (**1**)	C$_6$H$_5$Br	–COO^{t}Bu	6	49%	37,700
6	1.0 (**3**)	C$_6$H$_5$Br	–COO^{t}Bu	6	46%	41,800
7	1.0 (**1**)	4-MeOC$_6$H$_2$Br	–COO^{t}Bu	6	50%	38,500
8	1.0 (**3**)	4-MeOC$_6$H$_2$Br	–COO^{t}Bu	6	50%	45,500

[a] Reactions were performed with 1.0 equiv. of aryl halides and 1.3 equiv. of *tert*-butyl acrylate and 1.4 equiv of base in a DMF for required time at 120 °C. (TON = Turn Over Number).

Table 4
Summary of Suzuki coupling reaction results.

Entry[a]	Catalyst (mmol) × 10^{-5}	Substrates		Temp (°C)	Time h	Yield	TON
1	0.2 (**1**)	4-MeC$_6$H$_4$I	Boronic acid	50	8	89%	445,000
2	0.2 (**1**)	C$_6$H$_5$I	Boronic acid	50	8	70%	350,000
3	0.2 (**1**)	C$_6$H$_5$Br	Boronic acid	80	12	60%	300,000
4	0.2 (**1**)	4-MeOC$_6$H$_2$Br	Boronic acid	80	12	65%	325,000
5	0.4 (**3**)	4-MeC$_6$H$_4$I	Boronic acid	110	12	95%	237,500
6	0.4 (**3**)	C$_6$H$_5$I	Boronic acid	110	12	90%	225,000
7	0.4 (**3**)	C$_6$H$_5$Br	Boronic acid	110	12	80%	200,000
8	0.4 (**3**)	4-MeOC$_6$H$_2$Br	Boronic acid	110	12	60%	150,000

[a] Reactions were performed with 1.0 equiv. of aryl halides and 1.3 equiv. of boronic acid, 1.4 equiv. of base and 0.25 equiv. of Bu_4NBr in a H_2O:toluene (1:2) for required time at 50 °C or 80 °C or 110 °C (TON = Trun Over Number).

the color of the solution rapidly changed to reddish brown. The mixture was heated at 70 °C for 1.30 h while stirring, and then the resulting mixture was passed through celite. The volatiles were removed from the filtrate in vacuo to produce 132.6 mg (90%) of a red orange solid. ^{1}H NMR ($CDCl_3$): δ 6.82 (m, 2H, Ar–H), 6.48 (d, 2H, J = 2.4 Hz, Ar–H), 2.85 (s, 4H, $-CH_2CH_2-$), 2.55 (m, 4H, $-CH(Me)_2$), 1.42 (app. quartet (dvt), 12H, $-CH(Me)_2$), 1.27 (app. quartet (dvt), 12H, $-CH(Me)_2$). $^{31}P\{^1H\}$ NMR ($CDCl_3$): δ 49.53 (s). ^{13}C NMR ($CDCl_3$): δ 162.6, 160.9 (t), 135.8 (t), 135.4, 123.4 (t), 107.2 (t), 39.6 (s, $-CH_2CH_2-$), 25.1 (br s, $-CH(Me)_2$), 18.5 (s, $-CH(Me)_2$), 17.8 (s, $-CH(Me)_2$). Anal. Calcd. for $C_{26}H_{36}Br_2ClNP_2Pd$: C, 43.00; H, 5.00; N, 1.93. Found: C, 43.13; H, 4.89; N, 1.68.

X-ray data collection and refinement

Data collections were performed on an OXFORD XCALIBUR diffractometer, equipped with a CCD area detector, using graphite-monochromated Mo Kα (λ = 0.71073 Å) radiation and a low-temperature device [44]. All calculations were performed using SHELXS-97 and SHELXL-97 respectively using Olex 2-1.1 software package [45]. The structures were solved by direct methods and successive interpretation of the difference Fourier maps, followed by full-matrix least-squares refinement (against F2). All non-hydrogen atoms, except the disordered bromobenzene, were refined anisotropically. For complexes **1** and **3**, one of the bromobenzene is highly disordered and in complex **2**, the triflate ion is highly disorded, so additional calculation has been done by "SQUEEZE" option in PLATON [46,47]. The crystallographic figures have been generated using Olex 2-1.1 software package (50% probability thermalellipsoids).

Catalysis of the Heck coupling

To a 50 mL schlenk flask aryl halide (1 mmol), *tert*-butyl acrylate (1.2 mmol), Cs_2CO_3 (1.2 mmol) and 10 mL DMF were added. Then catalyst (complex **1** or **3**) 0.2–1.0 mmol% was added to the reaction mixture. The reaction vessel was placed into an oil bath and heated at 120 °C. After completion of the reaction, the crude reaction mixture was treated with water (50 mL) and ethyl acetate (50 mL). The organic layer was washed with 3 × 15 mL H_2O, dried over Na_2SO_4 and then filtered. The volatiles were removed in vacuo from the filtrate and dried at 70 °C.

Catalysis of Suzuki coupling

To 50 mL of Schlenk flask aryl bromide (10.0 mmol), boronic acid (12.0 mmol), K_2CO_3 (20.0 mmol), Bu_4NBr (2.0 mmol) and toluene: water (2:1) were added. Then catalyst (complex **1** or **3**) 0.2–0.3 mmol % was added to the reaction mixture. The reaction mixture was stirred for required time at 50 °C or 80 °C for catalyst **3** and 110 °C for catalyst **1**. The reaction mixture was treated with 20 mL of water and 50 mL of ethyl acetate and the organic layer was washed with 3 × 10 mL of water and dried over Na_2SO_4 and then filtered. The volatiles were removed in vacuo from the filtrate. Pure product was obtained by column chromatography.

Computational methods

The geometries of ligands **L1**, **L2** and complexes **1**, **2** and **3** have been fully optimized at B3LYP level of theory. The 6-311G** basis set [48] was used to describe H, C, N, Cl and Br. The Pd atom was described using the LANL2DZ basis set [49]. Vibrational frequency calculations have been performed on these optimized structures to confirm the stationary point. A solvent correction (toluene and DCM) was performed using the polarized continuum model (PCM). All these computational procedures have been used as implemented in the Gaussian-09 package [50].

Acknowledgment

Dr. C. S gratefully acknowledges the Council of Scientific and Industrial Research (CSIR), New Delhi, India for the financial support (No. 01(2535)/11/EMR-II) and Bhattacharya, S., Department of Chemistry, Pondicherry University, for solving the crystal data. K. Ramakrishna gratefully acknowledges the University Grants commission (**UGC**) for a Junior Research Fellowship. We thank the Central Instrumentation Facility, Pondicherry University, for NMR spectra and DST-FIST for the single-crystal X-ray diffraction facility.

Appendix A. Supplementary material

CCDC 950473 and 950472 contain the supplementary crystallographic data for this paper. These data can be obtained free of charge from The Cambridge Crystallographic Data Centre via www.ccdc.cam.ac.uk/data_request/cif.

Appendix B. Supplementary data

Supplementary data related to this article can be found at http://dx.doi.org/10.1016/j.jorganchem.2014.04.011.

References

[1] M. Gandelman, D. Milstein, Chem. Commun. (2000) 1603–1604.
[2] D.F. MacLean, R. McDonald, M.J. Ferguson, A.J. Caddell, L. Turculet, Chem. Commun. (2008) 5146–5148.
[3] B. Rybtchinski, A. Vigalok, Y. Ben-David, D. Milstein, J. Am. Chem. Soc. 118 (1996) 12406–12415.
[4] R. Cohen, M.E. van der Boom, L.J.W. Shimon, H. Rozenberg, D. Milstein, J. Am. Chem. Soc. 122 (2000) 7723–7734.
[5] M.E. van der Boom, S.-Y. Liou, Y. Ben-David, M. Gozin, D. Milstein, J. Am. Chem. Soc. 120 (1998) 13415–13421.
[6] M.E. van der Boom, S.-Y. Liou, Y. Ben-David, L.J.W. Shimon, D. Milstein, J. Am. Chem. Soc. 120 (1998) 6531–6541.
[7] F. Ozawa, T. Ishiyama, S. Yamamoto, S. Kawagishi, H. Murakami, M. Yoshifuji, Organometallics 23 (2004) 1698–1707.
[8] J. Choi, A.H.R. MacArthur, M. Brookhart, A.S. Goldman, Chem. Rev. 111 (2011) 1761–1779.
[9] L. Fan, L. Yang, C. Guo, B.M. Foxman, O.V. Ozerov, Organometallics 23 (2004) 4778–4787.
[10] B. Zou, H.-F. Jiang, Z.-Y. Wang, Eur. J. Org. Chem. 2007 (2007) 4600–4604.
[11] S. Bhattacharyya, T.J.R. Weakley, M. Chaudhury, Inorg. Chem. 38 (1999) 5453–5456.
[12] M.A. Esteruelas, J. García-Raboso, M. Oliván, E. Oñate, Inorg. Chem. 51 (2012) 5975–5984.
[13] S. Golisz, N. Hazari, J. Labinger, J. Bercaw, J. Org. Chem. 74 (2009) 8441–8443.
[14] X. Zhao, D. Liu, H. Guo, Y. Liu, W. Zhang, J. Am. Chem. Soc. 133 (2011) 19354–19357.
[15] N. Selander, K.J. Szabó, Chem. Rev. 111 (2010) 2048–2076.
[16] C.J. Moulton, B.L. Shaw, J. Chem. Soc. Dalton Trans. (1976) 1020–1024.
[17] M. van der Boom, D. Milstein, Chem. Rev. 103 (2003) 1759–1792.
[18] J. Cornella, E. Gómez-Bengoa, R. Martin, J. Am. Chem. Soc. 135 (2013) 1997–2009.
[19] J.A. Labinger, J.E. Bercaw, Nature 417 (2002) 507–514.
[20] D. Morales-Morales, R. Redon, C. Yung, C.M. Jensen, Chem. Commun. (2000) 1619–1620.
[21] B.L. Shaw, New J. Chem. 22 (1998) 77–79.
[22] R.B. Bedford, S.M. Draper, P. Noelle Scully, S.L. Welch, New J. Chem. 24 (2000) 745–747.
[23] E. Balaraman, C. Gunanathan, J. Zhang, L.J.W. Shimon, D. Milstein, Nat. Chem. 3 (2011) 609–614.
[24] R. Langer, G. Leitus, Y. Ben-David, D. Milstein, Angew. Chem. Int. Ed. 50 (2011) 2120–2124.
[25] G. Zhang, K.V. Vasudevan, B.L. Scott, S.K. Hanson, J. Am. Chem. Soc. 135 (2013) 8668–8681.
[26] J.L. Bolliger, O. Blacque, C.M. Frech, Angew. Chem. Int. Ed. 46 (2007) 6514–6517.
[27] T. Kimura, Y. Uozumi, Organometallics 25 (2006) 4883–4887.
[28] J.I. van der Vlugt, M.A. Siegler, M.I. Janssen, D. Vogt, A.L. Spek, Organometallics 28 (2009) 7025–7032.

[29] M. Gandelman, L.J.W. Shimon, D. Milstein, Chem. Eur. J. 9 (2003) 4295–4300.
[30] W. Weng, S. Parkin, O.V. Ozerov, Organometallics 25 (2006) 5345–5354.
[31] M.-H. Huang, L.-C. Liang, Organometallics 23 (2004) 2813–2816.
[32] R. Lindner, B. van den Bosch, M. Lutz, J.N.H. Reek, J.I. van der Vlugt, Organometallics 30 (2011) 499–510.
[33] L.-C. Liang, P.-S. Chien, P.-Y. Lee, Organometallics 27 (2008) 3082–3093.
[34] S. Chakraborty, J. Zhang, J. Krause, H. Guan, J. Am. Chem. Soc. 132 (2010) 8872–8873.
[35] D. Morales-Morales, C. Grause, K. Kasaoka, R.O. Redón, R.E. Cramer, C.M. Jensen, Inorg. Chim. Acta 300–302 (2000) 958–963.
[36] W. Weng, C. Guo, C. Moura, L. Yang, B.M. Foxman, O.V. Ozerov, Organometallics 24 (2005) 3487–3499.
[37] Y. Gloaguen, W. Jacobs, B. de Bruin, M. Lutz, J.I. van der Vlugt, Inorg. Chem. 52 (2013) 1682–1684.
[38] R.C. Bauer, Y. Gloaguen, M. Lutz, J.N.H. Reek, B. de Bruin, J.I. van der Vlugt, Dalton Trans. 40 (2011) 8822–8829.
[39] E.J. Derrah, S. Ladeira, G. Bouhadir, K. Miqueu, D. Bourissou, Chem. Commun. 47 (2011) 8611–8613.
[40] M.C. MacInnis, D.F. MacLean, R.J. Lundgren, R. McDonald, L. Turculet, Organometallics 26 (2007) 6522–6525.
[41] M. Mazzeo, M. Lamberti, A. Massa, A. Scettri, C. Pellecchia, J.C. Peters, Organometallics 27 (2008) 5741–5743.
[42] D. Adhikari, S. Mossin, F. Basuli, J.C. Huffman, R.K. Szilagyi, K. Meyer, D.J. Mindiola, J. Am. Chem. Soc. 130 (2008) 3676–3682.
[43] J.I. van der Vlugt, Eur. J. Inorg. Chem. 2012 (2012) 363–375.
[44] CrysAlisPro, Oxford Diffraction Ltd., Abingdon, U.K., 2010.
[45] G.M. Sheldrick, SHELXS-97 and SHELXL-97, University of Göttingen, Germany, 1997.
[46] A.L. Spek, Acta Crystallogr. Sect. D 65 (2009) 148–155.
[47] A.L. Spek, J. Appl. Crystallogr. 36 (2003) 7–13.
[48] A.D. Becke, J. Chem. Phys. 98 (1993) 5648–5652.
[49] P.J. Hay, W.R. Wadt, J. Chem. Phys. 82 (1985) 299–310.
[50] M.J. Frisch, G.W. Trucks, H.B. Schlegel, G.E. Scuseria, M.A. Robb, J.R. Cheeseman, G. Scalmani, V. Barone, B. Mennucci, G.A. Petersson, H. Nakatsuji, M. Caricato, X. Li, H.P. Hratchian, A.F. Izmaylov, J. Bloino, G. Zheng, J.L. Sonnenberg, M. Hada, M. Ehara, K. Toyota, R. Fukuda, J. Hasegawa, M. Ishida, T. Nakajima, Y. Honda, O. Kitao, H. Nakai, T. Vreven, J.A. Montgomery, J.E. Peralta, F. Ogliaro, M. Bearpark, J.J. Heyd, E. Brothers, K.N. Kudin, V.N. Staroverov, R. Kobayashi, J. Normand, K. Raghavachari, A. Rendell, J.C. Burant, S.S. Iyengar, J. Tomasi, M. Cossi, N. Rega, J.M. Millam, M. Klene, J.E. Knox, J.B. Cross, V. Bakken, C. Adamo, J. Jaramillo, R. Gomperts, R.E. Stratmann, O. Yazyev, A.J. Austin, R. Cammi, C. Pomelli, J.W. Ochterski, R.L. Martin, K. Morokuma, V.G. Zakrzewski, G.A. Voth, P. Salvador, J.J. Dannenberg, S. Dapprich, A.D. Daniels, Farkas, J.B. Foresman, J.V. Ortiz, J. Cioslowski, D.J. Fox, Wallingford CT, 2009.